Measuring order in the isotropic packing of elastic rods

2011 EPL 95 34002

(http://iopscience.iop.org/0295-5075/95/3/34002)

A Letters Journal Exploring the Frontiers of Physics

August 2011

EPL, **95** (2011) 34002
doi: 10.1209/0295-5075/95/34002

www.epljournal.org

Measuring order in the isotropic packing of elastic rods

E. Bayart[1], S. Deboeuf[1,2], F. Corson[1], A. Boudaoud[1,3] and M. Adda-Bedia[1(a)]

[1] *Laboratoire de Physique Statistique, Ecole Normale Supérieure, UPMC Paris 06, Université Paris Diderot, CNRS 24 rue Lhomond, 75005 Paris, France, EU*
[2] *Department of Physics, McGill University, 3600 University - Montréal (QC) H3A 2T8, Canada*
[3] *RDP, ENS Lyon - 46 allée d'Italie, 69007 Lyon, France, EU*

received 17 March 2011; accepted in final form 13 June 2011
published online 8 July 2011

PACS 46.32.+x – Static buckling and instability
PACS 46.70.Hg – Membranes, rods, and strings
PACS 61.43.-j – Disordered solids

Abstract – The packing of elastic bodies has emerged as a paradigm for the study of macroscopic disordered systems. However, progress is hampered by the lack of controlled experiments. Here we consider a model experiment for the isotropic two-dimensional confinement of a rod by a central force. We seek to measure how ordered is a folded configuration and we identify two key quantities. A geometrical characterization is given by the number of superposed layers in the configuration. Using temporal modulations of the confining force, we probe the mechanical properties of the configuration and we define and measure its effective susceptibility. These two quantities may be used to build a statistical framework for packed elastic systems.

Packed elastic objects are ubiquitous in Nature and technology. For instance, DNA is packed in the cell nucleous or in viral capsids [1,2], while growing tissues can be confined by their environment [3,4]. The optimization of folding is crucial in the design of self-deployable structures, such as tents or solar sails [5], or in waste disposal. Like a granular pile, a confined plate can be either in a crystalline state, the stacked facets obtained by repeatedly folding a sheet into two, or in a disordered state, exemplified by a crumpled ball [6]. When a sheet is confined, the number of metastable configurations blows up [7]. Meanwhile, self-avoidance leads to jamming because it prevents the system from exploring the space of configurations. This raises the question of whether a confined sheet can be viewed as a glassy system, in the same class as a static granular medium [8]. Indeed, theoretical studies proposed thermodynamical approaches for packed rods [2,9,10]. It has been argued that a system which is confined isotropically experiences a configurational phase transition from a disordered to an ordered (nematic) state [2,9]. The geometric characterization of the nematic ordering has been developed in various numerical and experimental works [6,10,11]. On the experimental side, a difficulty in the study of crumpled balls [11–16] arises from the hand-generation of configurations. In this context, the confinement of a rod in a plane was an important and useful simplification [7,17–20]. However, drawing general conclusions from these experiments can be questioned because of issues such as friction between the periphery of the configuration and the container, the anisotropic injection of the rod in the container, plasticity or the impossibility of unfolding a configuration.

Here we reconsider the packing of a rod in a plane by proposing an original model experiment. In addition to a geometric description of the transition from a disordered to an ordered configuration, we developed a mechanical characterization of the system allowing a global measure of the order without addressing the local geometrical properties of the folded configurations. To this purpose, we devised an experiment allowing us to reversibly confine a rod by a central force, deriving from an isotropic radial potential. As a consequence, there is no contact between the container and the periphery of the configuration, while the intensity of the forcing is controlled through the stiffness of the potential. We investigate the emergence of geometrical order through the stacking of layers. As this setup enables the temporal modulation of the confinement, we probe the mechanical properties of configurations, and define an effective susceptibility of a configuration, which we associate with geometrical order. We thus obtain a coupled geometrical and mechanical characterization of the system.

The principle of the experiment is as follows. A circular Hele-Shaw cell is filled with a liquid and entrained by a

(a) E-mail: adda@lps.ens.fr

motor. A rod is inserted into the cell. The cell is slightly thicker than the rod, so that the rod cannot cross itself, constraining a two-dimensional folding. The liquid is denser than the rod. As a consequence, when the cell is rotated, the rod is submitted to a centripetal force and thus confined in a radial, parabolic pressure potential $P(r) = P_0 + \rho\omega^2 r^2/2$, where r is the distance from the centre of the cell, ρ is the fluid density, ω is the angular velocity and P_0 is the pressure at the centre of the cell. We have checked that at the studied frequencies of rotation, gravitational effects become negligible. The cell was fixed in a vertical position on the axis of a 2 kW motor, through a double ball bearing to avoid vibration transmission from the motor to the cell. The rotation velocity was controlled using an electronic frequency variator. The flexible circular rod used in all experiments was made of PDMS (Goodfellow) and had the following characteristics: diameter $h = 2 \pm 0.2$ mm, total length $L = 3 \pm 0.01$ m, density $d = 1$ and Young Modulus $E = 1.0 \pm 0.1$ MPa (measured using a tensile testing method). The liquid was salt-saturated degassed water of density $\rho_l = 1.16$ at ambient temperature. The cell was made of three disks of 50 cm in diameter: a stiff one in 10 mm thick Duralumin (i), and two successive 15 mm thick transparent Polycarbonate disks (ii) and (iii), allowing us to observe the confined rod (fig. 1(a,b)). The two chambers communicate through two holes pierced in disk (ii) and were filled with the liquid through holes pierced in the edge of disks (i) and (iii). Chamber 2 is a sacrificial one: when the cell is rotated, the resulting pressure gradient in the liquid bends inwards disk (iii) but the gap is thick enough so that it does not close at our maximal rotation velocity of 20 Hz. Nevertheless, the pressure is equilibrated between the two faces of disk (ii) allowing to fix the gap throughout the whole spacing of chamber 1. The rod was gently inserted using a hole in the back of disk (i); the thickness of chamber 1 was fixed at 2.5 mm by a ring of Plexiglas inserted between disks (i) and (ii). The whole setup was placed in a dark room and lit with three stroboscopic lamps with diffusing screens. Movies were taken with a CCD camera. The duration of a flash was short enough (1 ms) to get sharp images of the rod, even at the highest velocities. Using a computer interface, the camera and stroboscopes were triggered with the same square periodic signal, while the variator was controlled using a DC voltage. To enhance contrast, we used a white rod on a dark back: an adhesive sheet of black plastic was laid on the Duralumin disk (i). Binary images of the rod were obtained by thresholding.

The initial configuration of the rod (fig. 1(a)) is prepared using 8 magnetic beads of diameter 1.8 mm inserted into the first chamber and moved from outside with a magnet. The cell is then set in rotation; the time to reach the desired frequency is approximately 3 s. The control parameter is the frequency of rotation $f = 2\pi\omega$. For a given frequency f, a large number of folded configurations is accessible from the same initial configuration (fig. 2). Indeed, the folding process is non-deterministic and the

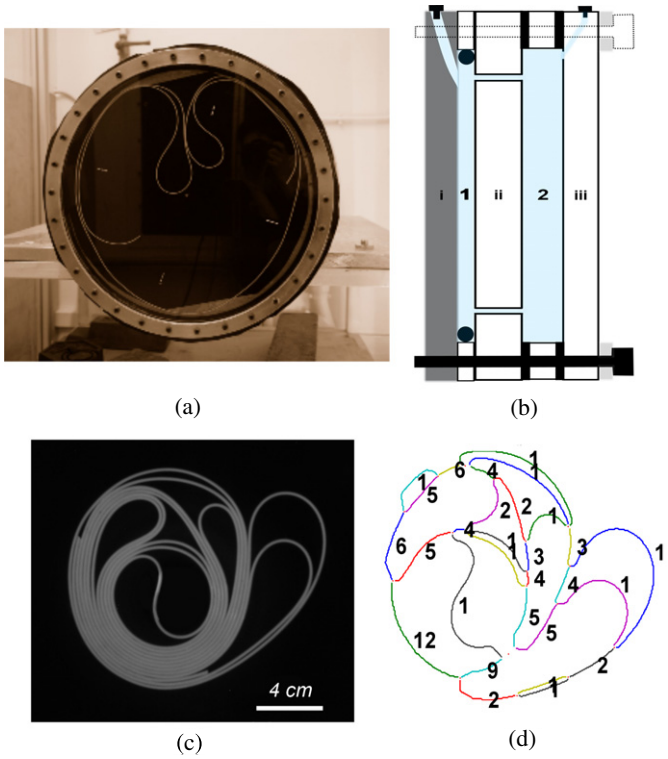

Fig. 1: (Colour on-line) The experiment. (a) A rod of density 1 is confined in a circular Hele-Shaw cell, filled with saturated salted water of density 1.16. The picture shows the rod in its initial configuration, before the cell has been set in rotation. (b) The cell is made of a superposition of three disks; the intermediate one (ii) is pierced with two holes to enable equilibration of pressure into the liquid. This setup enables to fix the thickness of chamber 1 where the rod is placed, chamber 2 being a sacrificial room. The chambers are made watertight with flat and toric joints shown in dark. (c) Example of an equilibrium configuration obtained when a centripetal force is generated by the rotation of the cell around its axis. (d) Corresponding skeletonized image in which the number of layers per branch is defined.

folded configuration is selected by the experimental noise at the very beginning of the experiment. We include in the noise the influence of friction between the rod and the disks and of fluid flow in the cell. During an experiment, the fluid is in solid rotation; the timescale of the transient flow to reach the solid rotation is of the order of 10^{-1} s which is much smaller than the time to reach equilibrium as it will be stated below. The second timescale to consider is the lubrification time needed to expulse fluid between the superposition of two segments of rod, which is of the order of 1 s, again much smaller than the experiment timescale.

First, the resulting configurations can be characterized using their radius of gyration,

$$R_g = \sqrt{\frac{1}{L}\int_0^L r^2(s)\,\mathrm{d}s},$$

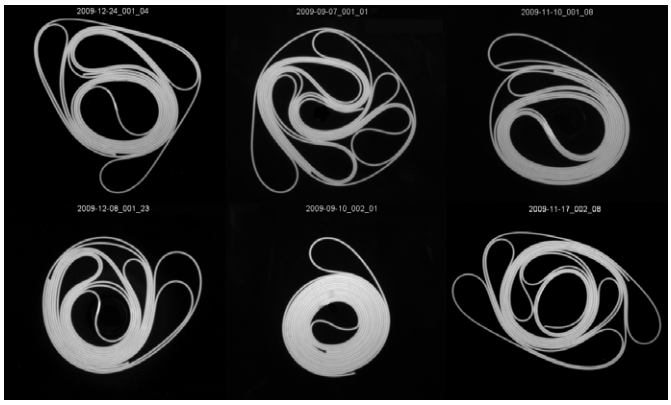

Fig. 2: Panel of folded configurations resulting from experiments with the same parameters. The rod is prepared in the initial configuration (fig. 1(a)) then the rotation frequency is increased from 0 to 12 Hz in approximately 3 s. The large variety of geometry shows that the folding is a non-deterministic process.

where s is the curvilinear coordinate of the rod and $r(s)$ the distance to the cell axis. This quantity is directly calculated using the binary image of the confined rod. The radius of gyration decreases with time, rapidly when the rotation is started (fig. 3(a)) and then more slowly, reaching a plateau value in a time lapse of the order of 10^3 s. This final value is not unique and differs according to realizations at a given frequency. As we only investigated equilibrium configurations, we had to wait 1800 s for each value of the frequency before taking measurements, to ensure that equilibrium is reached. When averaging over realizations, the mean radius of gyration $\bar{R}$ is found to be a decreasing function of confinement strength (fig. 3(b)). It appears that, when the same experiment is repeated, a large diversity of sizes and geometries is observed. The aim of the present study is to quantify geometrical order in equilibrium states. To do so, we extract the skeleton of a folded configuration from binary images, in which voids of area smaller than a given threshold have been filled. This thresholding process did not influence results. Vertices are detected as self-contact points, *i.e.* points of the skeleton having three neighbors (fig. 1(c), (d)). We define branches as portions delimited by two vertices. A given branch may contain several layers of the rod: the thickness of the branch on the binary image directly yields the number of layers. The analysis of the experimental patterns was coded allowing to treat a large number of data.

Inspired by observations (fig. 4(a)), we first consider a geometrical definition of order using the number of superposed layers. Indeed, the configuration of absolute minimum of energy is a spiral [7], which can be qualified as very ordered and in which all layers are superposed and contained in a unique branch. Experimentally, this number of superposed layers is defined as the average number of layers per branch in a given configuration. We jointly

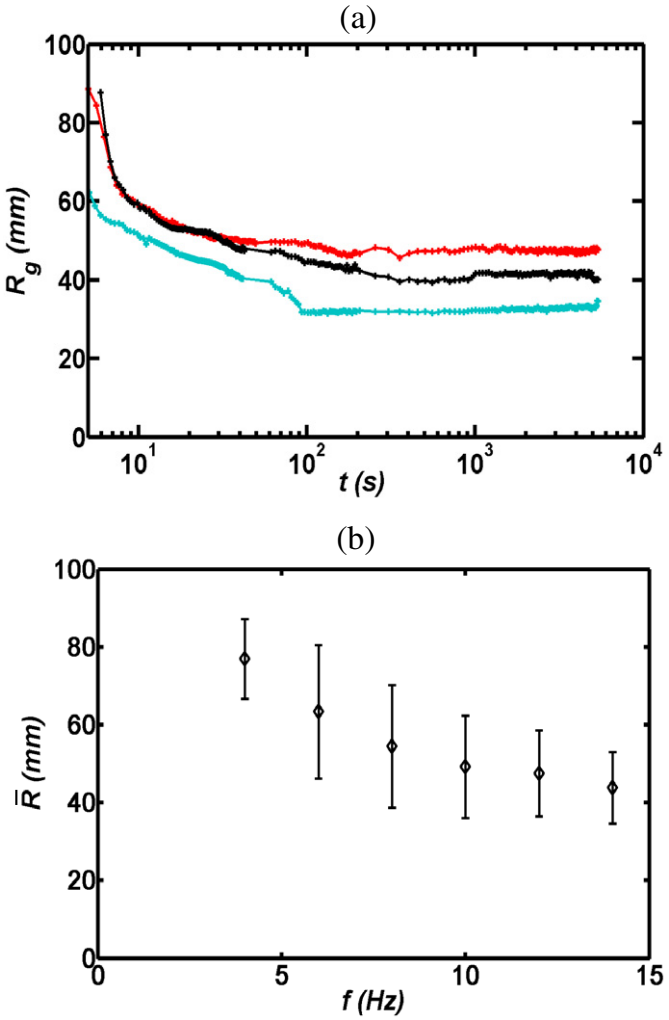

Fig. 3: (Colour on-line) The radius of gyration. (a) The radius of gyration R_g as a function of time for three realizations in which the cell was launched from 0 to 14 Hz in 3 s. Radii reach a plateau value in about 10^3 s. The final radius differs according to realizations. (b) On average, the radius of gyration $\bar{R}$ decreases with the strength of confinement (quantified by the rotation velocity, f of the disk). The bars represent widths of the distributions for each frequency of rotation.

measured the average number of layers per branch $\bar{N}_{l/b}$ and the radius of gyration of a configuration, as shown in fig. 4(b). The data roughly collapse on a single curve, independently of the confinement strength. Therefore, either the radius of gyration or the number of layers appear as better characterizations of the configuration. A disordered configuration, *i.e.* with small $\bar{N}_{l/b}$, has a larger radius than a spiral ordered configuration. As in some previous experiments [11,19,20], stacking appears as a distinctive feature of the confinement of rods, and our setup allows us to show that stacking decreases with the radius of the configuration. In the following we investigate the possibility of characterizing geometrical order without a detailed knowledge of the geometry of configuration. In other words, we seek an independent measure of order.

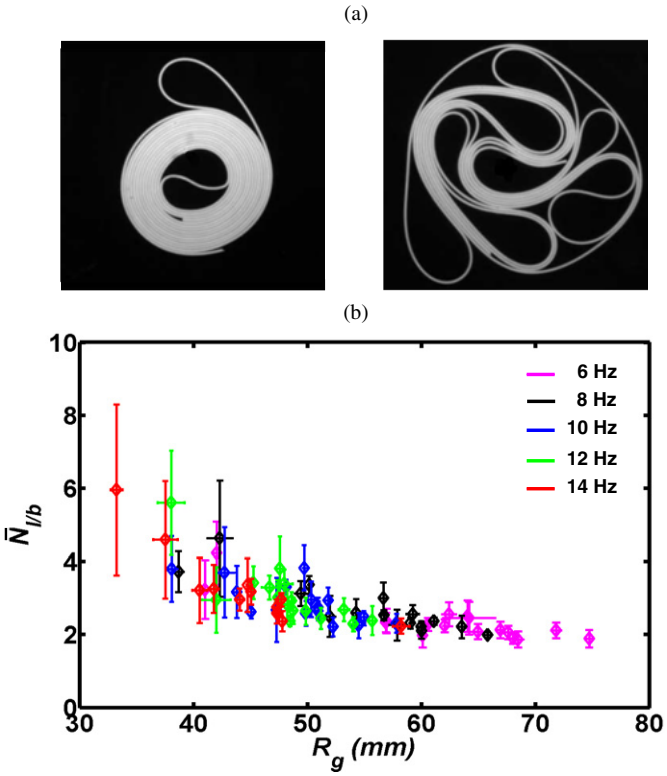

Fig. 4: (Colour on-line) Stacking. (a) Order and disorder. Two extreme examples of equilibrium configurations obtained at two different frequencies, with a large and a small number of superposed layers, respectively. (b) Average number of layers per branch, $N_{l/b}$, as a function of the radius of gyration R_g. Each point corresponds to one realization of the experiment. The colors of the symbols correspond to the imposed rotation velocity of the disk. An ordered configuration (large $N_{l/b}$) has a small radius of gyration.

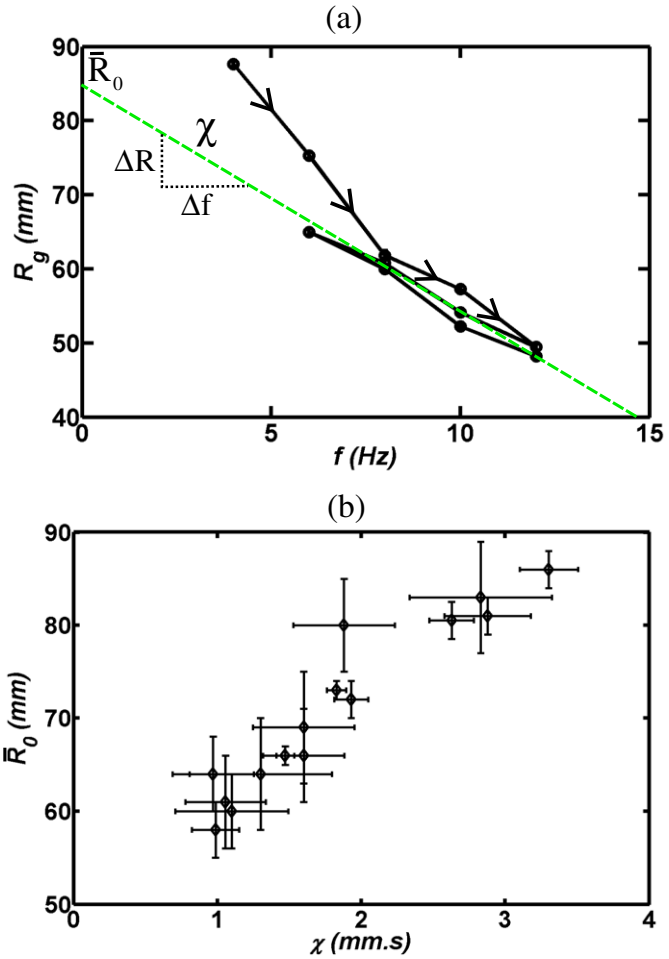

Fig. 5: (Colour on-line) Susceptibility. (a) Evolution of the radius of gyration R_g during an annealing experiment. After a first irreversible branch, the radius follows a reversible branch (parallel to the dashed line). A configuration is characterized by the slope of the line, χ, and its intercept, R_0, with the axis $f = 0$. (b) The characteristic radius R_0 as a function of susceptibility χ. Each point corresponds to one realization of an annealing experiment. The error bars correspond to the uncertainties estimates of the linear fits as described in (a).

We realized annealing experiments in which the confinement strength was repeatedly increased then decreased by varying the rotation velocity appropriately. At each step in rotation frequency, we waited 1800 s in order to reach equilibrium (fig. 3(a)), so that an annealing experiment typically took 12 hours. After a few frequency steps, the radius of gyration followed approximately the same line (fig. 5(a)). The first steps are irreversible, while the line is reversible. In other words, the system follows an irreversible branch in the (f, R_g) phase space before falling on a reversible branch. This behavior is reminiscent of the evolution of the density of a tapped granular pile according to the tapping acceleration, as reported in [21]. In our case, each annealing experiment can be characterized with the intercept, R_0, and with the slope, χ, of the reversible branch. Furthermore, we observed that no topological changes occurred along the reversible branch, as illustrated in fig. 6: the relative positions of loops remain constant, and the configuration only seems to breath. As a consequence a given annealing experiment leads to a well-defined configuration, which can be characterized with R_0 and χ. R_0 corresponds to its effective radius, while χ defines an effective susceptibility of the configuration as it measures its response to a variation in the strength of confinement. Here, the effective susceptibility is defined as the response of the system to an external field: the confinement potential. Thus, it is not the definition of the susceptibility used for glassy systems. When plotting these two quantities, the characteristic radius R_0 is found to be an increasing, roughly linear function of the susceptibility χ (fig. 5(b)). The results are independent of the confinement (frequency) since, whatever the annealing path, points seem to collapse on the same master curve. As we found above that an ordered configuration has a small radius of gyration (fig. 4(b)), this second set of results indicates that an ordered configuration has a small susceptibility, and, conversely, a disordered configuration is highly compressible. A possible interpretation is that

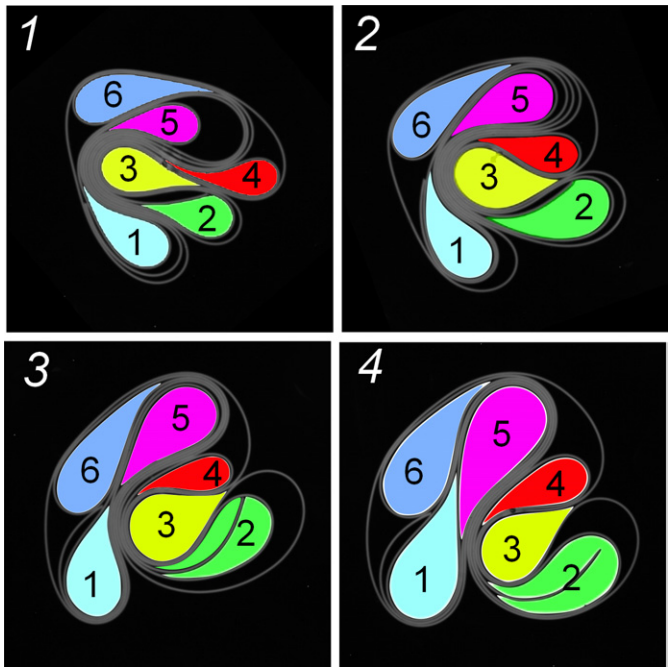

Fig. 6: (Colour on-line) Example of the evolution of a configuration during an annealing experiment. Rotation frequency was varied from 12 Hz (left) to 6 Hz (right), by steps of 2 Hz of 1800 s duration. Each colored area corresponds to a loop. The relative position of loops is invariant. The configuration only breathes under the perturbation.

self-avoidance imposes a stringent constraint on ordered configurations for which more stacking means less freedom in exploring phase space; as a consequence an ordered configuration would be less compressible. In mechanical terms, friction between layers is more important in an ordered configuration because contact area is larger. When confinement is decreased, unfolding is inhibited by friction.

To summarize, we built an experiment allowing the two-dimensional confinement of a rod in a parabolic potential. This experiment allowed us to quantify order and disorder in a configuration, using a geometrical measure of stacking and a mechanical measure of an effective susceptibility, this quantity being defined as the response of the system to an external field. We found that these two quantities are strongly correlated with the characteristic radius of the configuration. Although this effective susceptibility is strictly a response to variations in rotation velocity, it can be readily generalized to other 3D systems such as crumpled membranes. Indeed the definition and the measure of a nematic order in such systems are still unsolved issues. In that context, a salient feature of susceptibility is that its measurement does not require a full knowledge of the geometry of the configuration. In other words, order could be inferred from the effective stiffness of the crumpled ball. Future work should address whether these quantities could be used in a thermodynamic approach to packing, or how these quantities could emerge in such an approach. Thus geometrical and mechanical properties appear as strongly entangled in the packing of sheets and rods.

* * *

We are grateful to J. Da Silva Quintas for his help in building the experimental apparatus.

REFERENCES

[1] Arsuaga J., Vazquez M., Trigueros S., Sumners D. and Roca J., *Proc. Natl. Acad. Sci. U.S.A.*, **99** (2002) 5373.
[2] Katzav E., Adda-Bedia M. and Boudaoud A., *Proc. Natl. Acad. Sci. U.S.A.*, **103** (2006) 18900.
[3] D'Arcy-Thompson, *On Growth And Form* (Cambridge University Press, Cambridge) 1917.
[4] Couturier E., du Pont S. C. and Douady S., *PloS ONE*, **4** (2009) e7968.
[5] Miura K., *Proceedings of the 31st Congress of the International Astronautical Federation*, Vol. **IAF-80-A 31** (American Institute for Aeronautics and Astronautics, New York) 1980.
[6] Tallinen T., Aström J. A. and Timonen J., *Phys. Rev. Lett.*, **101** (2008) 106101.
[7] Boué L., Adda-Bedia M., Boudaoud A., Cassani D., Couder Y., Eddi A. and Trejo M., *Phys. Rev. Lett.*, **97** (2006) 166104.
[8] Jaeger H. M., Nagel S. R. and Behringer R. P., *Rev. Mod. Phys.*, **68** (1996) 1259.
[9] Boué L. and Katzav E., *EPL*, **80** (2007) 54002.
[10] Aristoff D. and Radin C., *EPL*, **91** (2010) 56003.
[11] Lin Y. C., Sun J. M., Hsiao J. H., Hwu Y., Wang C. L. and Hong T. M., *Phys. Rev. Lett.*, **103** (2009) 263902.
[12] Gomes M. A. F., *Am. J. Phys.*, **55** (1987) 649.
[13] Matan K., Williams R. B., Witten T. A. and Nagel S. R., *Phys. Rev. Lett.*, **88** (2002) 076101.
[14] Blair D. L. and Kudrolli A., *Phys. Rev. Lett.*, **94** (2005) 166107.
[15] Andresen C. A., Hansen A. and Schmittbuhl J., *Phys. Rev. E*, **76** (2007) 026108.
[16] Balankin A. S., Silva I. C., Martìnez O. A. and Huerta O. S., *Phys. Rev. E*, **75** (2007) 051117.
[17] Donato C. C., Gomes M. A. F. and de Souza R. E., *Phys. Rev. E*, **66** (2002) 015102.
[18] Stoop N., Wittel F. K. and Herrmann H. J., *Phys. Rev. Lett.*, **101** (2008) 094101.
[19] Deboeuf S., Adda-Bedia M. and Boudaoud A., *EPL*, **85** (2009) 24002.
[20] Adda-Bedia M., Boudaoud A., Boué L. and Deboeuf S., *J. Stat. Mech.* (2010) P11027.
[21] Nowak E. R., Knight J. B., Povinelli M. L., Jaeger H. M. and Nagel S. R., *Powder Technol.*, **94** (1997) 79.